THE JOURNAL OF PHYSICAL CHEMISTRY A

pubs.acs.org/JPCA

Article

Density Functional Theory Mechanistic Study on H_2O_2 Production Using an Organic Semiconductor Epindolidione

Nitin Wadnerkar, Viktor Gueskine,* Eric Daniel Głowacki, and Igor Zozoulenko*

Cite This: *J. Phys. Chem. A* 2020, 124, 9605–9610

Read Online

ACCESS | Metrics & More | Article Recommendations

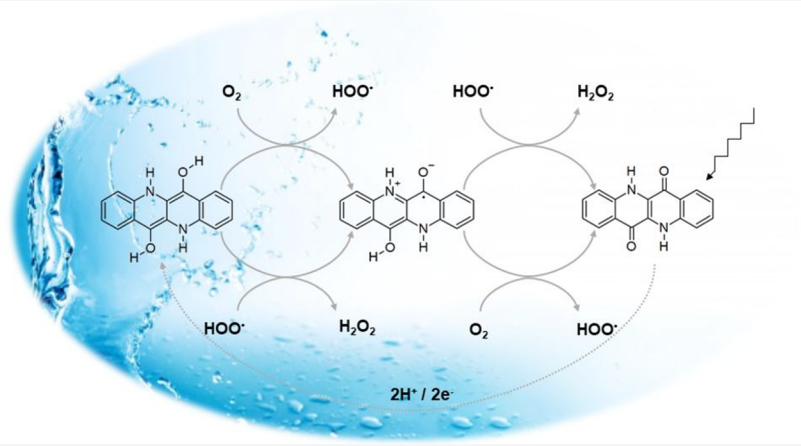

ABSTRACT: Organic semiconductors have recently emerged as promising catalytic materials for oxygen reduction to hydrogen peroxide, H_2O_2, a chemical of great importance in industry as well as biology. While examples of organic semiconductor-mediated photocatalytic and electrocatalytic processes for H_2O_2 production become more numerous and improve in performance, fundamental understanding of the reaction mechanisms at play have been explored far less. The aim of the present work is to computationally test hypotheses of how selective oxygen reduction to H_2O_2 generally occurs on carbonyl dyes and pigments. As an example material, we consider epindolidione (EPI), an industrial pigment with demonstrated semiconductor properties, which photocatalytic activity in oxygen reduction reaction (ORR) and thereby producing hydrogen peroxide (H_2O_2) in low pH environment has been recently experimentally demonstrated. In this work, the ability of the reduced form of EPI, viz. EPI-2H (which was formed after a photoinduced $2e^-/2H^+$ process), to reduce molecular triplet oxygen to peroxide and the possible mechanism of this reaction are computationally investigated using density functional theory. In the main reaction pathway, the reduction of O_2 to H_2O_2 reaction occurs via abstraction of one of the hydrogen atoms of EPI-2H by triplet dioxygen to produce an intermediate complex consisting of the radicals of hydrogen peroxide ($HOO^\bullet$) and EPI-$H^\bullet$ at the initial stage. $HOO^\bullet$ thus released can abstract another hydrogen atom from EPI-$H^\bullet$ to produce H_2O_2 and regenerates EPI; otherwise, it can enter another pathway to abstract hydrogen from a neighboring EPI-2H to form EPI-$H^\bullet$ and H_2O_2. EPI, after reduction, thus plays in ORR the role of hydrogen atom transfer (HAT) agent via its OH group, similar to anthraquinone in the industrial process, while HAT from its amino hydrogen is found unfavorable.

INTRODUCTION

Hydrogen peroxide (H_2O_2) is utilized extensively for water treatment,[1,2] chemical synthesis, and in the pulp and paper industry.[3] An emerging application of H_2O_2 is energy storage as a high energy density liquid fuel that can be used to drive fuel cells.[4−6] At present, most H_2O_2 is generated at an industrial scale through the oxidation process involving anthraquinone.[7] This complex process requires large plants and transportation of hazardous materials, significant energy input, and generates waste. The three key disadvantages are that this method requires input of H_2 gas, large volumes of organic solvents, and noble metal catalysts. The inherent complexity motivates researchers toward developing new concepts for direct production of H_2O_2, among which includes solar-to-fuel conversion via photochemical generation. For instance, generation of H_2O_2 from

Received: September 18, 2020
Revised: October 22, 2020
Published: November 9, 2020

https://dx.doi.org/10.1021/acs.jpca.0c08496
J. Phys. Chem. A 2020, 124, 9605–9610

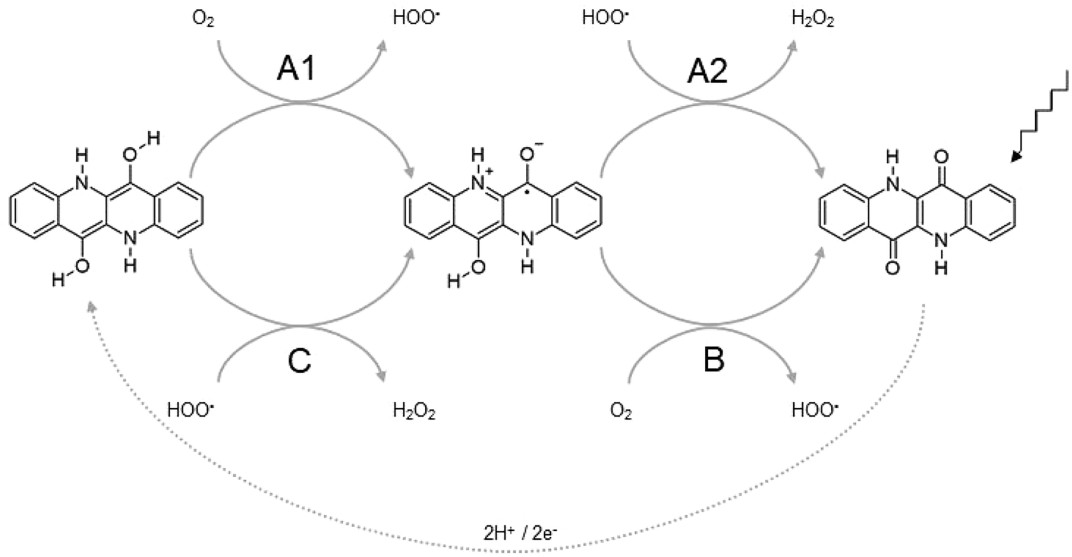

Figure 1. Proposed reaction pathways of O_2 reduction to H_2O_2 using EPI occurring at low pH.

O_2 and water is possible using graphitic carbon nitride (g-C_3N_4) by photocatalytic reductions,[8,9] though catalytic stability of these systems has not been tested.

In recent studies from our laboratory, H_2O_2 was produced by photocatalytic oxygen reduction reaction (ORR) at ambipolar organic semiconductors: low-cost hydrogen-bonded crystals of epindolidione (EPI) and quinacridone (QNC),[10] which are nontoxic and ecofriendly.[11,12] Of these two studied semiconductors, EPI was proven to be a more promising candidate for ORR, providing unique catalytic properties which exhibit performance that far exceeds that from previously reported inorganic semiconductors such as CdS and ZnO. Furthermore, it was subsequently shown that water-soluble analogues of these and other organic semiconductors are ORR photoactive in solution in the absence of aggregation.[13] Therefore, the roots of performance of these materials are to be sought at the molecular level. In the following, we concentrate on the role played by the EPI molecule in photochemical ORR.

EPI is a quinone, just like anthraquinone, and this chemical similarity invites us to compare the reactions of both these molecules leading to peroxide. The anthraquinone process comprises two distinct stages, whose mechanism was attentively studied theoretically only quite recently, though the process itself is quite old. First, anthraquinone is catalytically hydrogenated at a noble metal (Pd);[14] next, the anthrahydroquinone thus obtained is oxidized by molecular oxygen, yielding the target hydrogen peroxide and regenerating anthraquinone.[15] One can legitimately wonder why such a complex procedure was necessary and what is actually the role of anthraquinone. As discussed in a recent and very thorough theoretical study,[16] an enol or a phenol is among rare molecules that can ensure efficient hydrogen atom transfer (HAT) from the hydroxy group to molecular oxygen. Note that the formation of oxygen adduct intermediates has been considered and discarded in both refs 14 and 16. Indeed, the total spin conservation requirement imposes severe constraints on the mechanisms of reactions of triplet dioxygen with singlet molecules in particular (see ref 17 for a discussion). Specifically, direct dioxygen attachment to unsaturated bonds is actually spin-forbidden, as it would lead to very high-energy triplet products, intersystem crossing from a triplet to a singlet pathway being problematic. Therefore, the initial ORR step leading to hydrogen peroxide in the anthraquinone process consists in abstraction of an H atom by O_2.

Anthraquinone is also known to serve as an electrocatalyst in dark ORR to H_2O_2; when it is grafted onto a glassy carbon electrode,[18] we can reasonably suppose that HAT chemistry from the reduced (hydroquinone) form is at the origin of this electrocatalytic phenomenon.

The photochemical cycle with the participation of EPI is also separated in two distinct stages, though both take place in the same environment: (i) the photoelectrochemical stage of reductive hydrogenation of the EPI-quinone to EPI-biphenol: EPI + $2H^+$ + 2e → EPI-2H, (ii) the chemical reduction of molecular oxygen to hydrogen peroxide with regeneration of the quinone: EPI-2H + O_2 → EPI + H_2O_2.[10] The reaction sequence is apparently most similar to the anthraquinone process, and the advantage is the absence of the specific and costly heterogeneous catalyst for the first stage, allowing for the one-pot reaction. Taking for the time being the production of EPI-2H in the first stage for granted, we direct our attention in this work to the second, chemical ORR stage and use density functional theory (DFT) calculations to study whether its mechanism can be similar to that generally adopted for the anthraquinone process.

■ COMPUTATIONAL DETAILS

All calculations were performed using the Gaussian 09 package[19] with a range separated hybrid functional ωB97XD,[20] which comprises 100% long-range Hartree−Fock (HF) exact exchange, a small fraction (~22%) of short-range HF exact exchange, a modified B97 exchange density functional for short-range interaction, the B97 correlation density functional, and a model of Grimme's D2 dispersion corrections.[21] The 6-31G(d) basis set was used for all atoms. Here, we employed the SMD implicit aqueous solvation model for obtaining accurate solvation thermochemical properties. Transition states are located using the Berny algorithm.[22,23] All transition-state conformers manifested a single imaginary frequency. To arrive at free energies, the thermochemistry calculations herein were performed at a temperature of 298.15 K and pressure of 1 atm.

Reaction Schemes of ORR by the Reduced EPI-2H. As discussed above, we envisage HAT to triplet oxygen as the initial

https://dx.doi.org/10.1021/acs.jpca.0c08496
J. Phys. Chem. A 2020, 124, 9605−9610

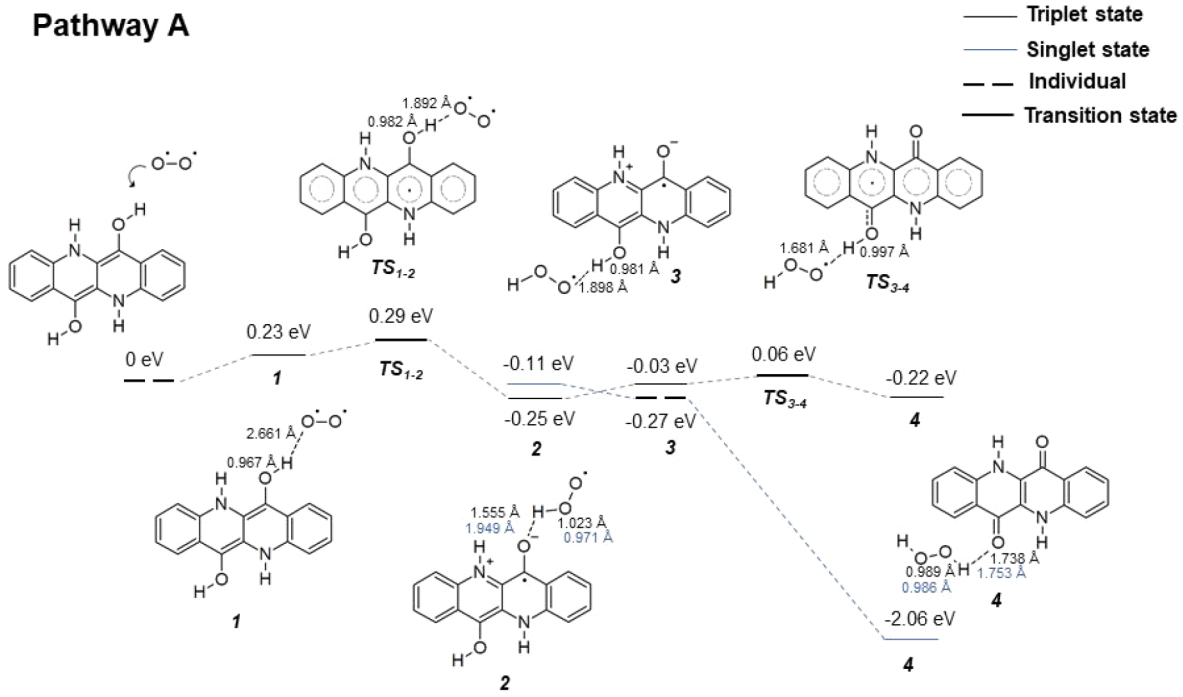

Figure 2. Potential energy profile and optimized geometries for the reaction pathway A of triplet O_2 to H_2O_2 production using photoreduced form of EPI (EPI-2H) in the singlet and triplet states. Bond lengths in black are for the triplet and in blue for the singlet states. The energy sum of individual solvated reactants is set as references for 0 eV energy.

stage of ORR by EPI-2H:[14,16] RH + $^3O_2$ → R$^\bullet$ + HOO$^\bullet$. The next question is which hydrogen could be thus donated by EPI-2H: that of its OH or NH group. Our preliminary calculation shows that the reaction with amino-hydrogen is endergonic with a solvated free energy change +0.22 eV. Therefore, participation of epindoline's amino-hydrogen in HAT can be practically excluded. This first result is in agreement with an important experimental finding[10] that the *N*-methylated derivative does conserve its ORR activity, even in the absence of NH groups. This leaves only hydroxo-hydrogen as a viable HAT candidate. The remaining possible HAT reactions are summarized in Figure 1, consecutively leading from molecular oxygen to H_2O_2 via HOO$^\bullet$ and regenerating EPI from EPI-2H via the monophenol radical EPI-H$^\bullet$. We consider the possibility of HAT from both bi- and monophenol to O_2 and HOO$^\bullet$. We are aware that HOO$^\bullet$ can also produce H_2O_2 by disproportionation (2HOO$^\bullet$ → H_2O_2 + O_2). In principle, all peroxide detected experimentally can form via this pathway; however, as our calculations will show, the catalytic cycle logically implicates a second reduction step mediated by EPI as a more probable route to H_2O_2.

RESULTS AND DISCUSSION

Reaction Pathway A (= A1 + A2). The free energy profile with the optimized geometries during the oxidation process of EPI-2H for the formation of hydrogen peroxide (H_2O_2) is shown in Figure 2. At the initial stage A1 (of the scheme in Figure 1), ^{1}EPI-2H is allowed to react with $^3O_2$ on a triplet potential energy surface, and we termed such individual reactants as "ind.react" for the respective reaction herein. At first, O_2 forms a weakly bound equilibrated reactant complex with EPI-2H **1** in a common solvent cage. As the reaction proceeds, O_2 directly abstracts a hydrogen atom from one of the enol groups of EPI-2H, thus forming HOȮ and EPI-Ḣ species of the intermediate **2**. In the produced EPI-Ḣ, an unpaired electron is found to be delocalized over the entire aromatic ring with negative charge on oxygen, whereas nitrogen nearby to it acquires positive charge in equal amount due to bond rearrangements, maintaining neutrality of this complex. It is noteworthy that the reaction (ind.react) → **1** → **2** is 0.25 eV exothermic and proceeds with the activation energy of only E_{act} = $E_{TS\ 1-2}$ − $E_{ind.react}$ = 0.29 eV (transition state TS_{1-2}). Therefore, it is remarkably facile, which indicates a high reductive capability of EPI-2H toward triplet dioxygen.

We note that intermediate **2** is practically degenerate with completely separated EPI-H$^\bullet$ and HOO$^\bullet$ (−0.27 eV), which indicates that the interaction between these is weak. EPI-H$^\bullet$ and HOO$^\bullet$ can thus easily separate. On the other hand, and for the same reason, a rearrangement of intermediate **2** viz. **3** in such a way that HOO$^\bullet$ just formed can abstract another hydrogen from the second enol unit of the same organic molecule, without leaving the solvent cage, should be easy. Such a rearrangement is required to enter stage A2 with the second HAT restoring EPI along with the generation of a H_2O_2 as the final products **4**. This process, still on the triplet potential surface, is found to be 0.22 eV exothermic and takes place via a transition state with the activation energy of only E_{act} = $E_{TS\ 3-4}$ − E_3 = 0.09 eV. As A1, A2 is thus favorable and facile. However, it should be understood that this entire triplet pathway is doomed, from some point on, to describe the electronically excited state of the system, as it does not lead to the products in the ground singlet state.

Therefore, we also investigated selected points of the singlet reaction pathway, starting from intermediate **2** toward the final products. Note that we have no computational access to the singlet counterparts of **2** and **3**, as these are open-shell singlets with essentially multideterminant wave function, not reliably described by conventional DFT.[24] Aware of this, we, nevertheless present the singlet intermediate **2** as an estimate. Indeed,

https://dx.doi.org/10.1021/acs.jpca.0c08496
J. Phys. Chem. A 2020, 124, 9605−9610

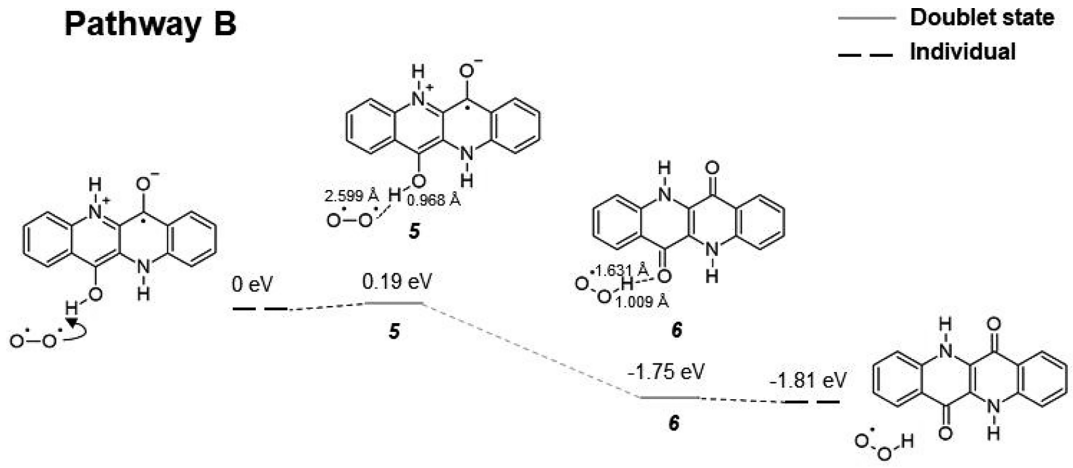

Figure 3. Potential energy profile and optimized geometries for the reaction pathway B for the oxidation of EPI-H$^{\bullet}$ by triplet O_2 in the doublet state. The energy sum of individual reactants is set as references for 0 eV energy.

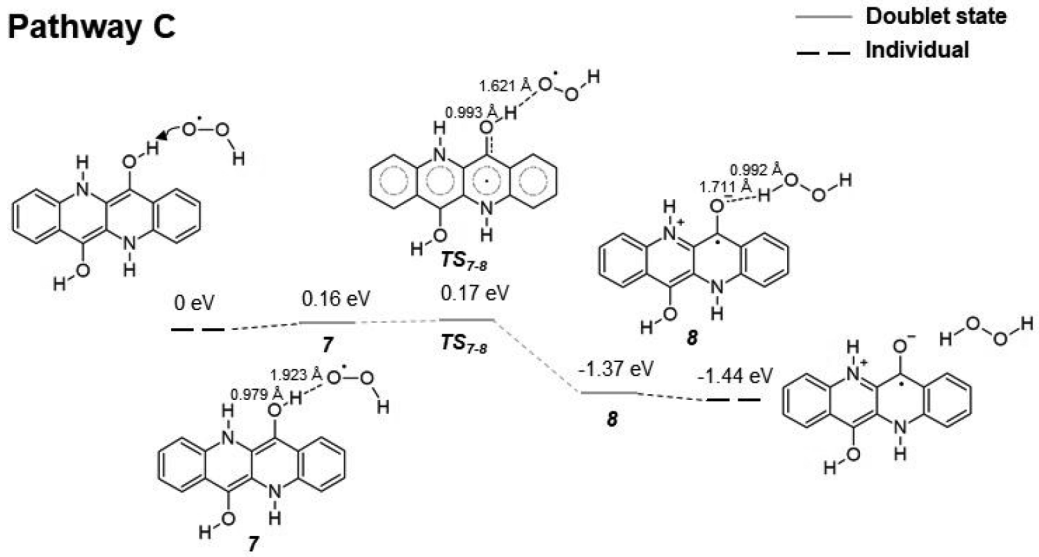

Figure 4. Potential energy profile and optimized geometries for the reaction pathway C for the oxidation of EPI-2H by HOO$^{\bullet}$ in doublet state. The energy sum of individual reactants is set as references for 0 eV energy.

the energy of isolated EPI-H$^{\bullet}$ and HOO$^{\bullet}$ (obviously the same for presumed singlet or triplet spin coupling between them at infinite separation) can be a good estimate of their singlet pair in a common solvent cage, as it is quasi-degenerate with their triplet complex. Also, this quasi-degeneracy suggests that the interconversion of weakly bound EPI-H$^{\bullet}$ and HOO$^{\bullet}$ can be presumed feasible, as it only requires the unpaired electrons of separated EPI-H$^{\bullet}$ and HOO$^{\bullet}$ to be recoupled with opposite spins. When the products **4** are in their ground singlet electronic state, their energy is much lower (−2.06 eV, relative to very initial reactants) than that achieved for a very similar geometry on the triplet potential surface. By comparing geometries and energies at the initial triplet and the final singlet pathways, it becomes clear that somewhere between **2** and **3** there lies their point of degeneracy, at which intersystem crossing becomes possible, though we are not in a position to estimate the probability of this event.

Reaction Pathway B. The energy profile in Figure 3 investigates HAT from the enol group of EPI-Ḣ intermediate, that can be produced at the stage A1, to $^3O_2$ on the doublet potential energy surface. As both reactants meet in a common solvent cage **5**, enol hydrogen abstraction takes place without any activation barrier, leading to the formation of products viz. EPI and HOO$^{\bullet}$ **6**, and the overall process is exothermic by 1.81 eV as the products are separated.

Reaction Pathway C. As we have demonstrated that ^{2}HOO$^{\bullet}$ species is generated via A1 or B, it is reasonable to inquire if this radical can abstract H from a neighboring ^{1}EPI-2H molecule, on the doublet potential surface, via the pathway C (see Figure 4). The energy profile C is found to resemble A2: HOO$^{\bullet}$ species abstracts hydrogen from a enol group of EPI-2H with activation energy of $E_{act} = E_{TS\ 1-2} - E_{ind.react} = 0.17$ eV, and this process is highly exothermic by −1.37 eV, with ^{2}EPI-H$^{\bullet}$ and $^1H_2O_2$ as products **8** through intermediate metastable complex 7.

CONCLUSION

Intrigued by the chemical similarity between EPI employed in a recently discovered photochemical production of hydrogen peroxide and anthraquinone, the workhorse of a well-established chemical industrial process, we were wondering if the

https://dx.doi.org/10.1021/acs.jpca.0c08496
J. Phys. Chem. A 2020, 124, 9605−9610

mechanisms of these processes could be similar. To arrive at H_2O_2 from O_2, two H obviously need to be attached to the latter, and the role of anthrahydroquinone (reduced anthraquinone) consists of providing them by two direct HATs. A number of hydroxyl-containing organic molecules were recently investigated for their HAT ability,[16] but reduced EPI was not among them. In the DFT calculations (including implicit water as solvent) presented above, we studied the interaction between molecular oxygen and EPI-2H as well as between the intermediates resulting after the first HAT. The overall mechanism presented herein is found analogous to the one proposed computationally for the industrial production of H_2O_2 in the anthraquinone reaction.[15] HAT is preceded by the formation of an intermediate complex between the reactants in a common solvent cage, thus preparing them for the target reaction. All of the possible HAT reactions with these are exothermic and, importantly, proceed with negligible activation barrier, being therefore thermodynamically and kinetically facile. These are free radical reactions starting with the triplet diradical molecular oxygen and passing via reactive radical intermediates. Such reactions usually involve a few pathways in parallel, and our results also suggest that there are a few possibilities to arrive at the target products. Importantly, the hydrogen atoms transferred to build up H_2O_2 originate only from the OH groups of the organic molecule. Indeed, we have observed that hydrogen attached to nitrogen could not participate in HAT, in agreement with the experimental result observed earlier.[10] EPI-2H thus belongs to the family of enols capable to ensure efficient transfer of hydrogen atoms to molecular oxygen via a radical mechanism. The role of the photochemical stage consists in generating reactive EPI-2H from the stable colorant EPI. Understanding these basics will hopefully be useful in designing efficient means to generate hydrogen peroxide from molecular oxygen. Knowing the significance of HAT is a key mechanistic insight which can allow screening of organic dyes and pigments to maximize this feature while balancing good optical and electronic properties.

AUTHOR INFORMATION

Corresponding Authors

Viktor Gueskine − *Laboratory of Organic Electronics, Department of Science and Technology, Linköping University, SE-60174 Norrköping, Sweden;* orcid.org/0000-0002-7926-1283; Email: viktor.gueskine@liu.se

Igor Zozoulenko − *Laboratory of Organic Electronics, Department of Science and Technology, Linköping University, SE-60174 Norrköping, Sweden;* orcid.org/0000-0002-6078-3006; Email: igor.zozoulenko@liu.se

Authors

Nitin Wadnerkar − *Laboratory of Organic Electronics, Department of Science and Technology, Linköping University, SE-60174 Norrköping, Sweden*

Eric Daniel Głowacki − *Laboratory of Organic Electronics, Department of Science and Technology and Wallenberg Centre for Molecular Medicine, Linköping University, SE-60174 Norrköping, Sweden; Faculty of Chemistry, Warsaw University of Technology, 00-664 Warsaw, Poland;* orcid.org/0000-0002-0280-8017

Complete contact information is available at: https://pubs.acs.org/10.1021/acs.jpca.0c08496

Notes

The authors declare no competing financial interest.

ACKNOWLEDGMENTS

The authors gratefully acknowledge financial support from the Knut and Alice Wallenberg Foundation through the project "H_2O_2", the Swedish Foundation for Strategic Research (SSF), the Swedish Research Council (2016-05990 and forskningsmiljö), and the Vinnova (Digital Cellulose Center and Treesearch). We are grateful for support from the National Science Centre, Poland, within grant 2019/33/B/ST5/01212. I.Z. thanks the Advanced Functional Material Center at Linköping University for support. The computations were performed on resources provided by the Swedish National Infrastructure for Computing (SNIC) at NSC and HPC2N.

REFERENCES

(1) Miglbauer, E.; Wójcik, P. J.; Głowacki, E. D. Single-Compartment Hydrogen Peroxide Fuel Cells with Poly(3,4-Ethylenedioxythiophene) Cathodes. *Chem. Commun.* **2018**, *54*, 11873−11876.

(2) Legrini, O.; Oliveros, E.; Braun, A. Photochemical Processes for Water Treatment. *Chem. Rev.* **1993**, *93*, 671−698.

(3) Hage, R.; Lienke, A. Applications of Transition-Metal Catalysts to Textile and Wood-Pulp Bleaching. *Angew. Chem., Int. Ed.* **2006**, *45*, 206−222.

(4) Disselkamp, R. S. Energy Storage Using Aqueous Hydrogen Peroxide. *Energy Fuels* **2008**, *22*, 2771−2774.

(5) Kato, S.; Jung, J.; Suenobu, T.; Fukuzumi, S. Production of Hydrogen Peroxide as a Sustainable Solar Fuel from Water and Dioxygen. *Energy Environ. Sci.* **2013**, *6*, 3756−3764.

(6) Yamada, Y.; Fukunishi, Y.; Yamazaki, S.-i.; Fukuzumi, S. Hydrogen Peroxide as Sustainable Fuel: Electrocatalysts for Production with a Solar Cell and Decomposition with a Fuel Cell. *Chem. Commun.* **2010**, *46*, 7334−7336.

(7) Campos-Martin, J. M.; Blanco-Brieva, G.; Fierro, J. L. Hydrogen Peroxide Synthesis: An Outlook Beyond the Anthraquinone Process. *Angew. Chem., Int. Ed.* **2006**, *45*, 6962−6984.

(8) Shiraishi, Y.; Kanazawa, S.; Sugano, Y.; Tsukamoto, D.; Sakamoto, H.; Ichikawa, S.; Hirai, T. Highly Selective Production of Hydrogen Peroxide on Graphitic Carbon Nitride (G-C3N4) Photocatalyst Activated by Visible Light. *ACS Catal.* **2014**, *4*, 774−780.

(9) Shiraishi, Y.; Kanazawa, S.; Kofuji, Y.; Sakamoto, H.; Ichikawa, S.; Tanaka, S.; Hirai, T. Sunlight-Driven Hydrogen Peroxide Production from Water and Molecular Oxygen by Metal-Free Photocatalysts. *Angew. Chem., Int. Ed.* **2014**, *53*, 13454−13459.

(10) Jakešová, M.; Apaydin, D. H.; Sytnyk, M.; Oppelt, K.; Heiss, W.; Sariciftci, N. S.; Głowacki, E. D. Hydrogen-Bonded Organic Semiconductors as Stable Photoelectrocatalysts for Efficient Hydrogen Peroxide Photosynthesis. *Adv. Funct. Mater.* **2016**, *26*, 5248−5254.

(11) Hunger, K. Toxicology and Toxicological Testing of Colorants. *Rev. Prog. Color. Relat. Top.* **2005**, *35*, 76−89.

(12) Herbst, W.; Hunger, K. *Industrial Organic Pigments: Production, Properties, Applications*; John Wiley & Sons, 2006.

(13) Gryszel, M.; Rybakiewicz, R.; Głowacki, E. D. Water-Soluble Organic Dyes as Molecular Photocatalysts for H2o2 Evolution. *Advanced Sustainable Systems* **2019**, *3*, 1900027.

(14) Kamachi, T.; Ogata, T.; Mori, E.; Iura, K.; Okuda, N.; Nagata, M.; Yoshizawa, K. Computational Exploration of the Mechanism of the Hydrogenation Step of the Anthraquinone Process for Hydrogen Peroxide Production. *J. Phys. Chem. C* **2015**, *119*, 8748−8754.

(15) Nishimi, T.; Kamachi, T.; Kato, K.; Kato, T.; Yoshizawa, K. Mechanistic Study on the Production of Hydrogen Peroxide in the Anthraquinone Process. *Eur. J. Org. Chem.* **2011**, *2011*, 4113−4120.

(16) Korth, H.-G.; Mulder, P. Phenolic Hydrogen Transfer by Molecular Oxygen and Hydroperoxyl Radicals. Insights into the Mechanism of the Anthraquinone Process. *J. Org. Chem.* **2020**, *85*, 2560−2574.

(17) Gueskine, V.; Singh, A.; Vagin, M.; Crispin, X.; Zozoulenko, I. Molecular Oxygen Activation at a Conducting Polymer: Electro-

chemical Oxygen Reduction Reaction at Pedot Revisited, a Theoretical Study. *J. Phys. Chem. C* **2020**, *124*, 13263−13272.
(18) Tammeveski, K.; Kontturi, K.; Nichols, R. J.; Potter, R. J.; Schiffrin, D. J. Surface Redox Catalysis for O2 Reduction on Quinone-Modified Glassy Carbon Electrodes. *J. Electroanal. Chem.* **2001**, *515*, 101−112.
(19) Frisch, M.; Trucks, G.; Schlegel, H.; Scuseria, G.; Robb, M.; Cheeseman, J.; Scalmani, G.; Barone, V.; Mennucci, B.; Petersson, G. *Gaussian 09*, Revision D. 01.; Gaussian, Inc.: Wallingford, 2013.
(20) Chai, J.-D.; Head-Gordon, M. Long-Range Corrected Hybrid Density Functionals with Damped Atom−Atom Dispersion Corrections. *Phys. Chem. Chem. Phys.* **2008**, *10*, 6615−6620.
(21) Grimme, S. Semiempirical Gga-Type Density Functional Constructed with a Long-Range Dispersion Correction. *J. Comput. Chem.* **2006**, *27*, 1787−1799.
(22) Peng, C.; Ayala, P. Y.; Schlegel, H. B.; Frisch, M. J. Using Redundant Internal Coordinates to Optimize Equilibrium Geometries and Transition States. *J. Comput. Chem.* **1996**, *17*, 49−56.
(23) Reed, A. E.; Weinhold, F. Natural Bond Orbital Analysis of near-Hartree−Fock Water Dimer. *J. Chem. Phys.* **1983**, *78*, 4066−4073.
(24) Gräfenstein, J.; Kraka, E.; Filatov, M.; Cremer, D. Can Unrestricted Density-Functional Theory Describe Open Shell Singlet Biradicals? *Int. J. Mol. Sci.* **2002**, *3*, 360−394.

https://dx.doi.org/10.1021/acs.jpca.0c08496
J. Phys. Chem. A 2020, 124, 9605−9610